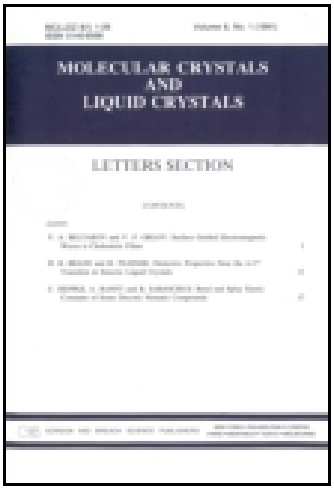

Molecular Crystals and Liquid Crystals
Publication details, including instructions for authors and subscription information:
http://www.tandfonline.com/loi/gmcl20

Theoretical Studies on the Electronic Structures and Phosphorescence Properties of Three Heteroleptic Cyclometalated Iridium(III) Complexes

Deming Han[a], Xiaohong Shang[b], Gang Zhang[c], Tian Li[a], Hongguang Li[a], Hongxing Cai[d], Xihe Zhang[d] & Lihui Zhao[a]

[a] School of Life Science and Technology, International Joint Research Center for Nanophotonics and Biophotonics, Changchun University of Science and Technology, Changchun, P. R. China

[b] College of Chemistry and Life Science, Changchun University of Technology, Changchun, P. R. China

[c] State Key Laboratory of Theoretical and Computational Chemistry, Institute of Theoretical Chemistry, Jilin University, Changchun, P. R. China

[d] School of Science, International Joint Research Center for Nanophotonics and Biophotonics, Changchun University of Science and Technology, Changchun, P. R. China

Published online: 08 Apr 2014.

To cite this article: Deming Han, Xiaohong Shang, Gang Zhang, Tian Li, Hongguang Li, Hongxing Cai, Xihe Zhang & Lihui Zhao (2014) Theoretical Studies on the Electronic Structures and Phosphorescence Properties of Three Heteroleptic Cyclometalated Iridium(III) Complexes, Molecular Crystals and Liquid Crystals, 591:1, 74-85, DOI: 10.1080/15421406.2013.822755

To link to this article: http://dx.doi.org/10.1080/15421406.2013.822755

Mol. Cryst. Liq. Cryst., Vol. 591: pp. 74–85, 2014

ISSN: 1542-1406 print/1563-5287 online
DOI: 10.1080/15421406.2013.822755

Theoretical Studies on the Electronic Structures and Phosphorescence Properties of Three Heteroleptic Cyclometalated Iridium(III) Complexes

DEMING HAN,[1] XIAOHONG SHANG,[2] GANG ZHANG,[3] TIAN LI,[1] HONGGUANG LI,[1] HONGXING CAI,[4] XIHE ZHANG,[4] AND LIHUI ZHAO[1,*]

[1]School of Life Science and Technology, International Joint Research Center for Nanophotonics and Biophotonics, Changchun University of Science and Technology, Changchun, P. R. China
[2]College of Chemistry and Life Science, Changchun University of Technology, Changchun, P. R. China
[3]State Key Laboratory of Theoretical and Computational Chemistry, Institute of Theoretical Chemistry, Jilin University, Changchun, P. R. China
[4]School of Science, International Joint Research Center for Nanophotonics and Biophotonics, Changchun University of Science and Technology, Changchun, P. R. China

The geometry structures, electronic structures, absorption, and phosphorescence properties of three heteroleptic cyclometalated iridium(III) complexes have been theoretically investigated by the density functional theory (DFT) method. The highest occupied molecular orbital (HOMO) of the three complexes has the similar distributions on two main ligands. However, the lowest unoccupied molecular orbital (LUMO) of the three complexes has different distributions on different ligand fragments. Especially for 3, the LUMO is mainly composed of the picolinate auxiliary ligand. The lowest lying absorptions were calculated to be at 409, 473, and 414 nm for 1–3, respectively. By changing the conjugation length of the main ligand from 1 to 2, one can tune the emission color from green to red. The addition of sterically bulky phenolic substituents in ***3*** *also results in an obvious red shift of the emission wavelength. The calculated results show that the absorption and emission transition character can be changed by altering the main ligands. Calculations of ionization potential (IP) and electron affinity (EA) were used to evaluate the injection abilities of holes and electrons into these complexes. The theoretical work should provide a suitable guide to the future design and synthesis of novel phosphorescent materials for use in the organic light-emitting diodes (OLEDs).*

[Supplemental materials are available for this article. Go to the publisher's online edition of Molecular Crystals and Liquid Crystals to view the free supplemental file.

Keywords Absorption; DFT; emission; iridium; phosphorescence

*Address correspondence to Lihui Zhao, School of Life Science and Technology, International Joint Research Center for Nanophotonics and Biophotonics, Changchun University of Science and Technology, Changchun 130022, Jilin, P. R. China+86-431-85583023; +86-431-85583099. E-mail: zhaolh@cust.edu.cn

1. Introduction

Since Forrest *et al*. used PtOEP as a phosphorescent dopant to greatly improve organic light-emitting diode (OLED) efficiencies in 1998, a number of heavy metal complexes, such as iridium, platinum, ruthenium, osmium, copper, etc., have been investigated [1–5]. Among them, iridium(III) complexes have exhibited tremendous potential in the area of optoelectronic applications, especially as triplet dopant emitters in OLEDs [6–9]. The high thermal stability and short lifetime in excited states could reduce the probabilities of triplet–triplet annihilation and increase photoluminescent (PL) quantum efficiencies [10–13]. Theoretical investigations showed that the highest occupied molecular orbital (HOMO) of $Ir(F_2\text{-}ppy)_2L$ (L denotes ancillary ligand) complexes consists of a mixture of phenyl π- and Ir *d*-orbital, and the lowest unoccupied molecular orbital (LUMO) is localized largely on the pyridyl π^*-orbital [14,15]. Thus, a generally used strategy to tune emission color to red relies on the introduction of electron-donating groups to the phenyl moiety or extending the π-conjugation length of ppy, which can elevate the HOMO energy levels more than that of LUMO by increasing the $d\pi$ composition and therefore narrow the HOMO–LUMO gaps [16–18]. As is known, the phosphorescence wavelength, quantum yields, and electroluminescent efficiency of phosphorescent complexes are closely related to the π-conjugation length of the cyclometalated ligand, substitution positions, and substituent inductive effect. To obtain ideal emitters in OLEDs, the modification of cyclometalated and/or ancillary ligands is used to tune the emission colors over the entire visible spectra [19–21]. Recently, Gu *et al*. [22] have done a theoretical study of complex FIrpic. Yang *et al*. have theoretically investigated the phosphorescent properties of a series of Ir(III) complexes with the different ancillary ligand, including FIrpic, FIrmpic, FIrpca, and FIrprza [23].

On the basis of the most widely studied complex **1** (FIrpic), we propose two artificial structures 2 and 3 by altering the main ligand 2-(2,4-difluorophenyl)pyridine moiety. The electronic structures, charge injection, and transport, and spectral properties of these complexes have been calculated by the density functional theory (DFT) method. It is anticipated that the theoretical results could provide useful information for these experimentalists in synthesizing new phosphors in OLED.

2. Computational Details

The ground state geometry for each molecule was optimized by the DFT [24] method with Becke's three-parameter hybrid method combined with the Lee–Yang–Parr correlation functional (denoted as B3LYP) [25,26]. The geometry optimizations of the lowest triplet states (T_1) were performed by unrestricted B3LYP approach. On the basis of the ground- and excited state equilibrium geometries, the time-dependent DFT (TDDFT) approach was applied to investigate the absorption and emission spectral properties. The "double-ξ" quality basis set LANL2DZ [27,28] associated with the pseudopotential was employed on Ir atom. The 6–31G(d) basis set was used for nonmetal atoms in the gradient optimizations. Furthermore, the stable configurations of these complexes can be confirmed by frequency analysis, in which no imaginary frequency was found for all configurations at the energy minima. In addition, the positive and negative ions with regard to the "electron–hole" creation are relevant to their use as OLED materials. Thus, ionization potentials (IPs), electron affinities (EAs), and reorganization energy (λ) were obtained by comparing the energy levels of neutral molecule with positive ions and negative ions, respectively. All calculations were performed with the Gaussian 09 software package [29].

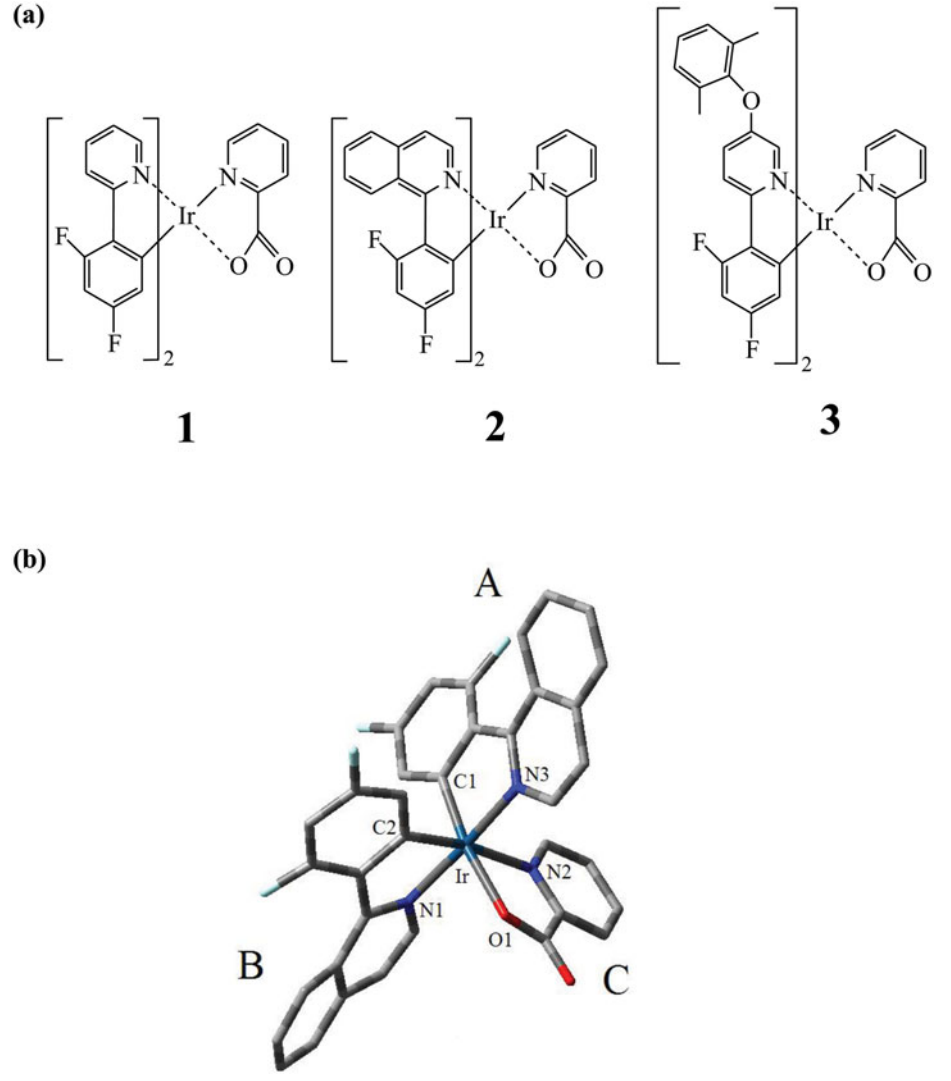

Figure 1. (a) The schematic structures for the studied complexes **1–3**. (b) Optimized structures of **2** in the ground states (the hydrogen atoms are omitted for clarity).

3. Results and Discussion

3.1. Geometric Structures and Molecular Orbital Properties

The sketch map of the three heteroleptic cyclometalated iridium(III) complexes **1–3** is presented in Fig. 1(a) and the optimized ground state geometric structure for **2** is shown in Fig. 1(b) along with the numbering of some key atoms, which can be named as A, B, and C. The main structural parameters of **1–3** in the ground and lowest triplet states (T_1) are shown in Table 1. These optimized Ir(III) complexes show a distorted octahedral geometry with two main ligands and one picolinate auxiliary ligand around iridium atom.

Table 1. The key optimized geometry parameters for **1–3** in the ground and excited triplet states

	1		2		3	
	S_0	T_1	S_0	T_1	S_0	T_1
			Bond length (Å)			
Ir–C1	2.0111	1.9814	2.0008	1.9938	2.0113	1.9895
Ir–C2	2.0130	2.0019	2.0098	2.0073	2.0148	2.0082
Ir–N1	2.0723	2.0888	2.0757	2.0888	2.0722	2.0866
Ir–N2	2.2108	2.2569	2.2127	2.2253	2.2083	2.2350
Ir–N3	2.0621	2.0439	2.0618	2.0299	2.0605	2.0359
Ir–O1	2.1796	2.1673	2.1822	2.1815	2.1840	2.1768
			Bond angle (deg)			
C1–Ir–N3	80.43	82.06	79.88	81.23	80.63	81.77
C1–Ir–N2	97.60	94.53	95.95	95.83	97.30	96.03
C1–Ir–O1	171.54	168.82	170.44	170.65	171.29	170.33
N1–Ir–N3	175.46	176.17	174.60	175.39	175.32	175.67
C2–Ir–N2	171.00	171.23	171.32	172.16	171.21	171.50

It is seen that the bond lengths of Ir−O1 for **1–3** gradually increase, that is, 2.1796 Å for **1**, 2.1822 Å for **2**, and 2.1840 Å for **3**. Compared with S_0 state, their T_1 state geometry structures change slightly. For the three complexes, the Ir−C1, Ir−C2, Ir−N3, and Ir−O1 bond lengths decrease from S_0 to T_1 state. In contrast, the Ir−N1 and Ir−N2 bond lengths increase from S_0 to T_1 state. These dihedral angles also show different change from S_0 to T_1 state.

It is known that the frontier molecular orbitals (FMOs) of the ground states (S_0) are very important because they are closely related to spectral properties, especially HOMO and LUMO. The HOMO and LUMO distribution, energy levels, and energy gaps between the LUMO and HOMO ($\Delta E_{L–H}$) of the three complexes **1–3** are plotted in Fig. 2. The calculated FMO compositions for **1–3** were presented in Tables S1–S3 (supplemental material). For **1**, Fig. 2 and Table S1 show that the HOMO, at −5.47 eV, distributes over the *d*-orbital of Ir (41%) and the two main ligand moieties (52%), with negligible composition from ancillary ligand moiety. The HOMOs of **2** and **3** have the similar orbital composition to that of **1**. For **1**, the LUMO is localized on one main ligand (26%) and ancillary ligand (73%). It is different for **2** and **3** that the LUMOs are localized on one main ligand (89%) and ancillary ligand (95%), respectively. The emission color tuning by grafting various substituents relies on the fact that the lowest excited state is relatively well described as a transition from HOMO to LUMO in a given ligand. Therefore, the investigation on the $\Delta E_{L–H}$ will give some useful information on the variation trend of absorption and emission spectra. Figure 2 shows that the extended π-conjugation length in **2** can stabilize the LUMO energy by 0.37 eV and increase the HOMO energy by 0.07 eV, therefore resulting in the narrow $\Delta E_{L–H}$ (3.31 eV) compared with the 3.75 eV for **1**. For **3**, the stronger inductive effect of phenol also leads to the slightly narrow $\Delta E_{L–H}$ (3.69 eV) compared to **1**. There will be an electronic transition from the HOMO to the LUMO or LUMO+1 for **1** in the lowest singlet transitions. However, for **2** and **3**, the HOMO→LUMO transition may be

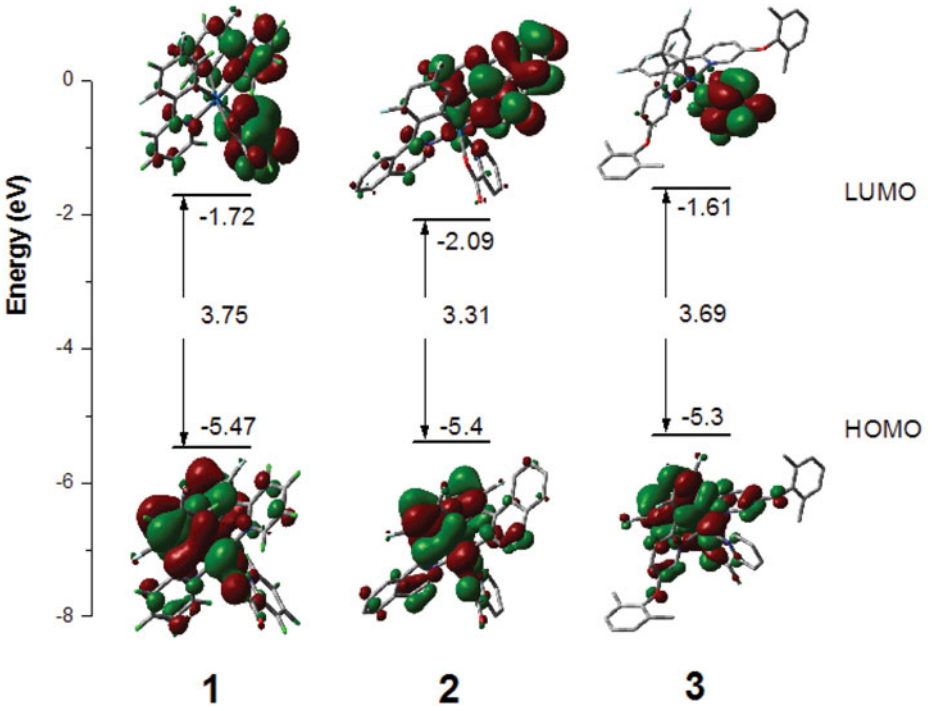

Figure 2. Molecular orbital diagrams and HOMO and LUMO energies for complexes **1–3**.

the dominant character. Considering the configuration of OLEDs, proper energy matching between host and dopants is an essential issue. Different HOMO and LUMO energies will have a significant effect on hole and electron injection balance and the position of the recombination zone, as well as device performance, which will be discussed in the next paragraph.

3.2. Ionization Potentials (IPs) and Electronic Affinities (EAs)

In this section, IPs, EAs, and reorganization energy (λ) have been calculated for complexes **1–3**, together with hole extraction potential (HEP) and electron extraction potential (EEP). The IP and EA can be either for vertical excitations (v; at the geometry of neutral molecule) or adiabatic excitations (a; optimized structure for both the neutral and charged molecules). The IPs and EAs are used to evaluate the energy barrier for the injection of holes and electrons.

In Table 2, the calculated IPs decrease in the following order **1**→**2**→**3**, which implies that the difficulties of hole injection from the hole-transporting layer (HTL) to these complexes gradually decrease in the order **1**→**2**→**3**. The smaller IP for **3** indicates easier injection of holes into the emitting materials from the HTL. By analysis of the EA value, **2** more easily accepts an electron than **1** and **3**, and this trend is also consistent with the order of LUMO energy levels. The large EA value for **2** indicates easier injection of electrons into the emitting materials from the electron-transporting layer.

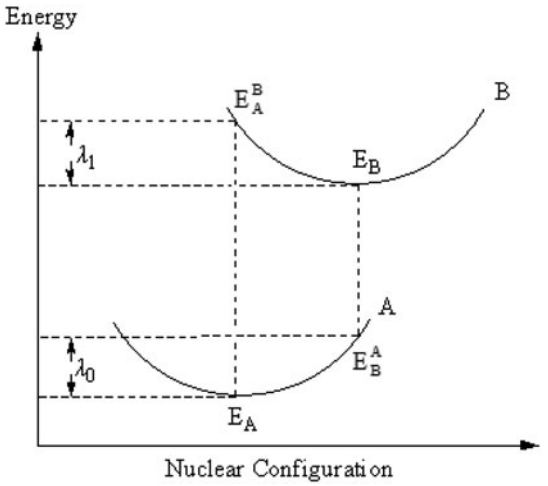

Figure 3. Schematic description of internal reorganization energy for hole transfer.

According to the Marcus–Hush model [30–32], the charge (hole or electron) transfer rate K_{et} can be expressed by the following formula:

$$K_{et}=A\exp(-\lambda/4k_BT), \tag{1}$$

where T is the temperature, k_B is the Boltzmann constant, and λ is the reorganization energy. Due to the limited intermolecular charge transfer range in the solid state, the mobility of charges has been demonstrated to be predominantly related to the internal reorganization energy λ for OLED materials [33–36]. Thus, at constant temperature, a low λ value is required for an efficient charge transport process. Herein, we focus on the inner reorganization energy λ_i, which is caused by the change of the internal nuclear coordinates from the reactant A to the product B and vice versa (Fig. 3). It can be expressed by the following formula:

$$\lambda_i = \lambda_0 + \lambda_1 = (E_B^A - E_A) + (E_A^B - E_B), \tag{2}$$

where E_A and $E_A^B$are the energies of A and B at the optimized geometry of A, respectively; $E_B^A$and E_B are the energies of A and B at the optimized geometry of B, respectively. The hole and electron injection and transport balance is important to emitting layer materials.

Table 2. Ionization potentials (IPs; eV), electron affinities (EAs; eV), and reorganization energies (eV) data for complexes **1**–**3**

	IP_v	IP_a	EA_v	EA_a	HEP	EEP	λ_{hole}	$\lambda_{electron}$
1	6.68	6.55	0.50	0.58	6.38	0.66	0.30	0.16
2	6.52	6.42	0.96	1.04	6.28	1.13	0.24	0.17
3	6.43	6.30	0.41	0.52	6.14	0.64	0.29	0.22

Table 3. Selected calculated wavelength (nm), oscillator strength (f), major contribution, transition characters, and the available theoretical wavelength (nm) for complexes **1–3** (H indicates HOMO, L indicates LUMO)

	State	λ/E	f	Configuration	Assignment	Nature	Theor[a]
1	S_1	409/3.02	0.0304	H→L+1 (48%)	d(Ir)+π(A+B)→π^*(A+C)	MLCT/LLCT	424
				H→L (47%)	d(Ir)+π(A+B)→π^*(A+C)	MLCT/LLCT	
	S_8	339/3.64	0.0612	H-1→L+2 (83%)	d(Ir)+π(B+C)→π^*(B)	MLCT/LLCT	
	S_{21}	297/4.17	0.0582	H-5→L+1 (45%)	d(Ir)+π(A)→π^*(A+C)	MLCT/LLCT	
	S_{26}	285/4.34	0.0569	H-1→L +5 (54%)	d(Ir)+π(B+C)→π^*(B+C)	MLCT/LLCT	
	S_{27}	283/4.36	0.0739	H-3→L+3 (31%)	d(Ir)+π(A+B)→π^*(A+C)	MLCT/LLCT	
2	S_1	473/2.61	0.0503	H→L (96%)	d(Ir)+π(A+B)→π^*(A)	MLCT/LLCT	
	S_5	387/3.19	0.0672	H-1→L+1 (86%)	d(Ir)+π(B)→π^*(B)	MLCT/LLCT	
	S_{13}	341/3.62	0.1043	H-4→L (31%)	π(B+C)→π^*(A)	LLCT	
	S_{14}	334/3.70	0.0898	H-5→L (52%)	d(Ir)+π(A+C)→π^*(A)	MLCT/LLCT	
	S_{25}	298/4.15	0.0916	H-1→L+4 (74%)	d(Ir)+π(B)→π^*(A)	MLCT/LLCT	
3	S_1	414/2.99	0.0012	H→L (94%)	d(Ir)+π(A+B)→π^*(C)	MLCT/LLCT	
	S_8	338/3.66	0.0661	H-1→L+2 (67%)	d(Ir)+π(B)→π^*(B)	MLCT/LLCT	
	S_{18}	307/4.02	0.0628	H-5→L (69%)	d(Ir)+π(A)→π^*(C)	MLCT/LLCT	
	S_{25}	289/4.28	0.0653	H-4→L+3 (37%)	π(C)→π^*(A+C)	LLCT	
	S_{27}	285/4.34	0.1642	H-1→L+5 (28%)	d(Ir)+π(B)→π^*(B)	MLCT/LLCT	

[a]Ref. [23].

The low reorganization energy is necessary for an efficient charge transport process. The calculated reorganization energies for hole transport (λ_{hole}) are obviously larger than electron transport ($\lambda_{electron}$), which indicates that electron-transporting performance of these complexes is better than the hole-transporting performance. Complex **2** has the best hole transfer ability with the smallest λ_{hole} value with respect to other two complexes. Moreover, the energy difference between λ_{hole} and $\lambda_{electron}$ for **2** (0.07 eV) is small, which can greatly improve the charge transfer balance, thus further enhancing the device performance of OLEDs.

3.3. Absorption Spectra

The absorption properties of complexes **1–3** have been investigated on the basis of the optimized ground state geometries. The vertical electronic excitation energies, oscillator strengths (f), dominant configurations, and their assignments have been listed in Table 3. The stimulated absorption spectra of the studied complexes based on the TDDFT calculations are shown in Fig. 4.

Table 3 shows that the calculated lowest lying absorption bands exhibit red shifting in the following order: **1** (409 nm) → **3** (414 nm) → **2** (473 nm), consistent with the variation rules of the ΔE_{L-H}. It can be seen that the calculated value of 409 nm for **1** is in good agreement with the theoretical result by Yang *et al.* [23]. As expected, the S_1 state comes from the HOMO→LUMO/LUMO+1 transition for **1**, and the HOMO→LUMO transition contributes to the S_0→S_1 state for **2** and **3**. As a result of the negligible intensity for **3** (0.0012), the S_0→S_1 transition is probably forbidden and would be practically absent in the

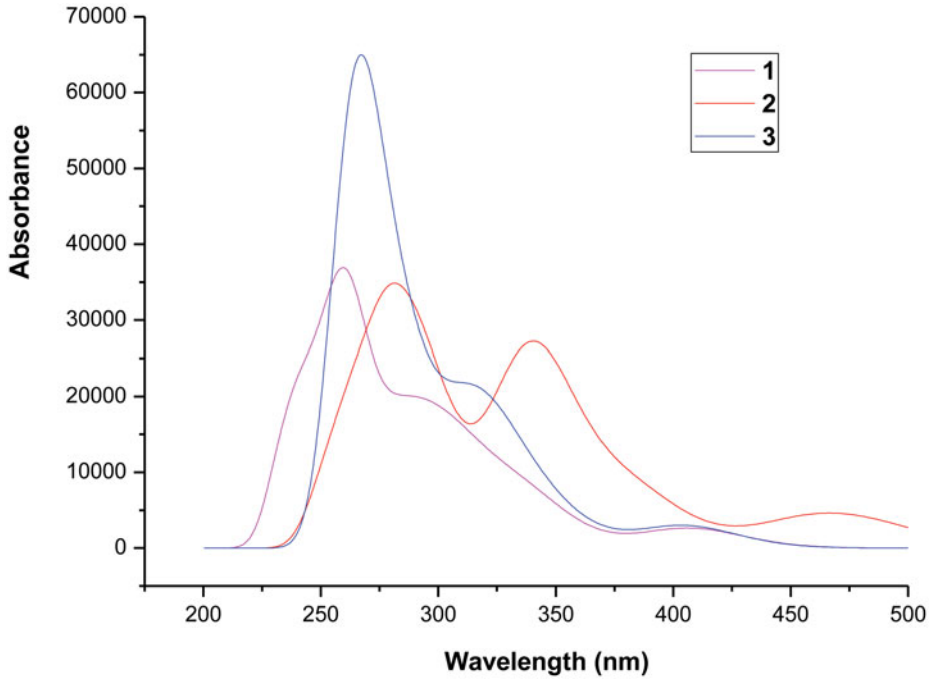

Figure 4. Simulated absorption spectra for complexes **1–3**.

absorption spectra. From the above discussion on FMO, the calculated 409 nm absorption for **1** can be described as the $d(\mathrm{Ir})+\pi(\mathrm{A+B})\rightarrow\pi^*(\mathrm{A+C})$ transition with the character of metal-to-ligand charge transfer (MLCT) and ligand-to-ligand charge transfer (LLCT). The 473 and 414 nm absorptions for **2** and **3** can be contributed by the $d(\mathrm{Ir})+\pi(\mathrm{A+B})\rightarrow\pi^*(\mathrm{A})$ and $d(\mathrm{Ir})+\pi(\mathrm{A+B})\rightarrow\pi^*(\mathrm{C})$ transition, respectively. For **3**, there is a larger absorption peak at about 285 nm dominated by one intense excitation ($f = 0.1642$). From Table 3, it can be seen that all the important transitions with the greatest oscillation strengths are not attributed by HOMO−LUMO transition.

3.4. Phosphorescence

On the basis of the optimized triplet excited state (T_1) geometries, the emission properties of complexes **1–3** obtained using the TDDFT method are shown in Table 4. The plots of the molecular orbitals related to emissions of **1–3** are also presented in Fig. 5.

Table 4 shows that the calculated lowest energy emissions are localized at 544 (2.27 eV), 786 (1.57 eV), and 573 (2.16 eV) nm for **1–3**, respectively. The predicted emission wavelength deviates from the experimental result by 44 nm for **1** [37]. The reason for the large difference of emission may be attributed to the limitations of the TDDFT method as shown by Katarzyna Świderek *et al*. [38], that is, high-energy excitations are not described by the TDDFT method. The oscillator strengths for phosphorescent emissions are also zero due to the without-spin-orbit coupling (SOC) effect in TDDFT results. One possible reason is that the excited state geometry we used here was optimized in the gas phase, and another reason is the limited dimensions of the basis set. For these

Table 4. Calculated emission wavelengths (nm)/energies (eV) and dominant orbital emissions from TDDFT results for complexes **1–3** (H indicates HOMO, L indicates LUMO)

	λ (nm)/*E* (eV)	Configuration	Assign	Exptl.[a]
1	544/2.27	L→H (73%)	LMCT/LLCT/ILCT [π^*(A)→*d*(Ir)+π(A+C)]	500 nm
		L→H-2 (18%)	LMCT/LLCT/ILCT	
		L→H-2 (18%)	[π^*(A)→*d*(Ir)+π(A+C)]	
2	786/1.57	L→H (56%)	LMCT/LLCT/ILCT [π^*(A)→*d*(Ir)+π(A+C)]	
		L→H-1 (35%)	LMCT/LLCT/ILCT [π^*(A)→*d*(Ir)+π(A+B)]	
3	573/2.16	L→H (64%)	LMCT/LLCT/ILCT [π^*(A+B)→*d*(Ir)+π(A+B)]	
		L→H-1 (23%)	LMCT/LLCT/ILCT [π^*(A+B)→*d*(Ir)+π(A+B)]	

[a]Ref. [37].

emissions of **1–3**, the configurations are contributed by the LUMO→HOMO$_{-n}$ (n = 0, 1, 2). For example, the phosphorescence emission at 786 nm of **2** is mainly from the transitions of LUMO→HOMO(56%) and LUMO→HOMO-1(35%) configuration. For the three complexes, their emission transition characters are assigned to LMCT(ligand-to-metal charge transfer)/LLCT(ligand-to-ligand charge transfer)/ILCT(intraligand charge transfer). For example, the emission of **2** has LMCT/LLCT/ILCT[π^*(A)→*d*(Ir)+π(A+C)] and LMCT/LLCT/ILCT[π^*(A)→*d*(Ir)+π(A+B)] characters as shown in Fig. 5. The calculated Stokes shifts between the lowest-lying absorptions and emissions are 0.48, 0.67, 0.56 eV for **1–3**, respectively. In these complexes, the main ligand has strong chelate interaction with the center metal Ir atom. The general metalcentered (MC) excited state can be greatly destabilized and, consequently, reduce the deactivation through this process. It is obvious that the frontier molecular orbital compositions are responsible for the emissions. The transition characters of the other complexes have also been analyzed and listed in Table 4.

The emission quantum yield (Φ) can be affected by the competition between k_r (radiative decay rate) and k_{nr} (nonradiative decay rate), that is, $\Phi = k_r/(k_r + k_{nr})$. Hence, to increase the quantum yield, k_r should be increased and k_{nr} should be decreased simultaneously or respectively [39,40]. A larger ^{3}MLCT composition and thus the intersystem crossing (ISC) can increase the phosphorescence quantum efficiencies. The direct involvement of the *d*(Ir) orbital enhances the first-order SOC in the $T_1 \rightarrow S_0$ transition, resulting in a drastic decrease of the radiative lifetime and an increased nonradiative rate constant. The calculated ^{3}MLCT contributions are 30.24%, 30.45%, and 27.87% for **1, 2,** and **3**, respectively. Besides, it is also known that the phosphorescence quantum efficiencies are inversely proportional to the $\Delta E_{S_1-T_1}$ [41]. A minimal $\Delta E_{S_1-T_1}$ is required for enhancing the ISC rate, leading to the increased k_r. The $\Delta E_{S_1-T_1}$ for complexes **1–3** are 0.399, 0.713, and 0.582 eV, respectively.

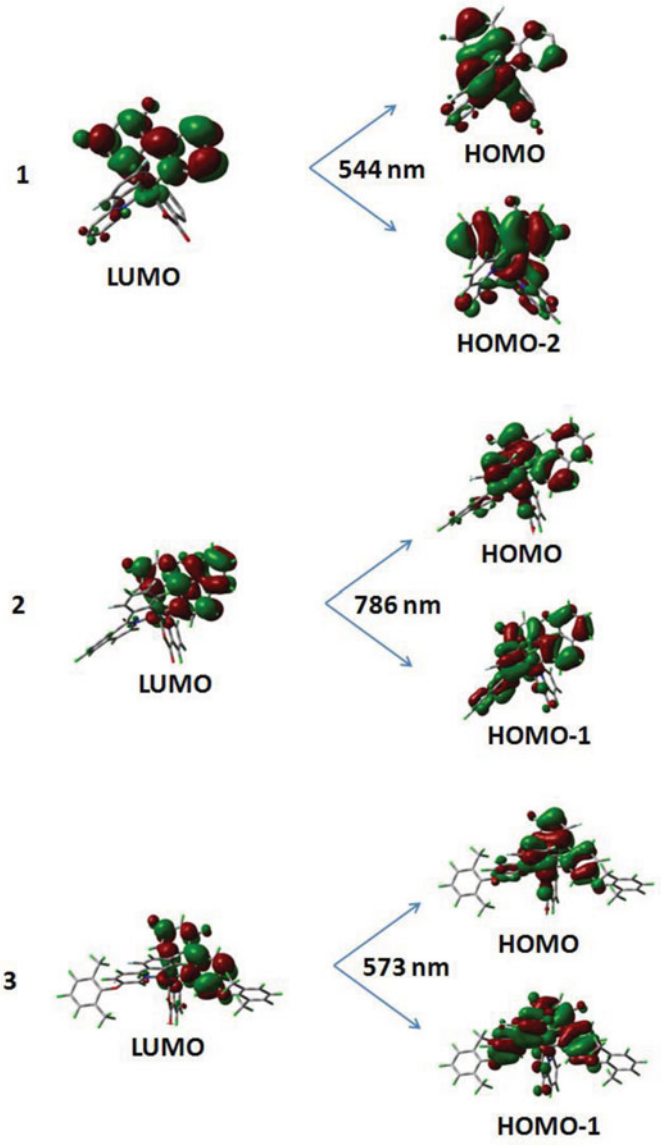

Figure 5. Transitions responsible for the emissions at 544, 786, and 573 nm for complexes **1–3**, respectively.

4. Conclusions

In this study, we have applied DFT and TDDFT methods to investigate the geometry structures, electronic structures, absorption, and phosphorescence properties of three heteroleptic cyclometalated iridium(III) complexes with different main ligands. The lowest lying absorptions were calculated to be at 409, 473, and 414 nm for **1–3**, respectively, and have the transition configuration of HOMO→LUMO or HOMO→LUMO+1. The lowest lying transitions can be assigned as metal/ligand to ligand charge transfer (MLCT/LLCT).

The calculated lowest energy emissions occur at 544 (2.27 eV), 786 (1.57 eV), and 573 nm (2.16 eV) for **1–3**, respectively, with the transition character of LMCT/LLCT/ILCT. Ionization potential, EAs, and reorganization energy were obtained to evaluate the charge transfer and balance properties between hole and electron. Among the three complexes, **2** has the best hole transfer ability with the smallest λ_{hole} value. In addition, the small energy difference between λ_{hole} and $\lambda_{electron}$ for **2** can greatly improve the charge transfer balance, thus further enhancing the device performance of OLEDs. We hope that these theoretical studies can provide some revelatory information in designing good phosphorescent materials for OLED applications.

Acknowledgments

The authors are grateful to the financial aid from the Program of Science and Technology Development Plan of Jilin Province (grant no. 20110438) and the Funds for Doctoral Scientific Research Startup of Changchun University of Science and Technology (grant no. 40301855).

References

[1] Indelli, M. T., Carli, S., Ghirotti, M., Chiorboli, C., Ravaglia, M., Garavelli, M., & Scandola, F. (2008). *J. Am. Chem. Soc.*, *130*, 7286.
[2] Costa, R. D., Céspedes-Guirao, F. J., Orti, E., Bolink, H. J., Gierschner, J., Fernández-Lázaro, F., & Sastre-Santos, A. (2009). *Chem. Commun.*, *26*, 3886.
[3] Chen, J. L., Chi, Y., Chen, K., Cheng, Y. M., Chung, M. W., Yu, Y. C., Lee, G. H., Chou, P. T., & Shu, C. F. (2010). *Inorg. Chem.*, *49*, 823.
[4] Park, S. W., Ham, H. W., & Kim, Y. S. (2011). *Mol. Cryst. Liq. Cryst.*, *551*, 24.
[5] Shang, X. H., Han, D. M., Li, D. F., & Wu, Z. J. (2013). *Chem. Phys. Lett.*, *565*, 12.
[6] Mi, B. X., Wang, P. F., Gao, Z. Q., Lee, C. S., Lee, S. T., Hong, H. L., Chen, X. M., Wong, M. S., Xia, P. F., Cheah, K. W., Chen, C. H., & Huang, W. (2008). *Adv. Mater.*, *20*, 1.
[7] Smith, A. R. G., Ruggles, J. L., Cavaye, H., Shaw, P. E., Darwish, T. A., James, M., Gentle, I. R., & Burn P. L. (2011). *Adv. Funct. Mater.*, *21*, 2225.
[8] Wang, R. J., Deng, L. J., Zhang, T., & Li, J. Y. (2012). *Dalton Trans.*, *41*, 6833.
[9] Tan, G. P., Chen, S. M., Sun, N., Li, Y. H., Fortin, D., Wong, W. Y., Kwok, H. S., Ma, D. G., Wu, H. B., Wang, L. X., & Harvey, P. D. (2013). *J. Mater. Chem. C*, *1*, 808.
[10] Baldo, M. A., Adachi, C., & Forrest, S. R. (2000). *Phys. Rev. B*, *62*, 10967.
[11] Adachi, C., Baldo, M. A., Thompson, M. E., & Forrest, S. R. (2001). *J. Appl. Phys.*, *90*, 5048.
[12] Reineke, S., Walzer, K., & Leo, K. (2007). *Phys. Rev. B*, *75*, 125328.
[13] Staroske, W., Pfeiffer, M., Leo, K., & Hoffmann, M. (2007). *Phys. Rev. Lett.*, *98*, 197402.
[14] Byun, Y., Jeon, W. S., Lee, T. W., Lyu, Y. Y., Chang, S., Kwon, O., Han, E., Kim, H., Kim, M., Lee, H. J., & Das, R. R. (2008). *Dalton Trans.*, 4732.
[15] Ashizawa, M., Yang, L., Kobayashi, K., Sato, H., Yamagishi, A., Okuda, F., Harada, T., Kuroda, R., & Haga, M. (2009). *Dalton Trans.*, 1700.
[16] Hay, P. J. (2002). *J. Phys. Chem. A*, *106*, 1634.
[17] Lowry, M. S., Hudson, W. R., Pascal, R. A., Jr., & Bernhard, S. (2004). *J. Am. Chem. Soc.*, *126*, 14129.
[18] Zhao, Q., Liu, S. J., Shi, M., Wang, C. M., Yu, M. X., Li, L., Li, F. Y., Yi, T., & Huang, C. H. (2006). *Inorg. Chem.*, *45*, 6152.
[19] Hwang, F. M., Chen, H. Y., Chen, P. S., Liu, C. S., Chi, Y., Shu, C. F., Wu, F. I., Chou, P. T., Peng, S. M., & Lee, G. H. (2005). *Inorg. Chem.*, *44*, 1344.
[20] Li, J., Djurovich, P. I., Alleyne, B. D., Yousufuddin, M., Ho, N. N., Thomas, J. C., Peters, J. C., Bau, R., & Thompson, M. E. (2005). *Inorg. Chem.*, *44*, 1713.

[21] Zhou, G. J., Ho, C. L., Wong, W. Y., Wang, Q., Ma, D. G., Wang, L. X., Lin, Z. Y., Marder, T. B., & Beeby, A. (2008). *Adv. Funct. Mater.*, *18*, 499.
[22] Gu, X., Fei, T., Zhang, H., Xu, H., Yang, B., Ma, Y., & Liu, X. (2008). *J. Phys. Chem. A*, *112*, 8387.
[23] Yang, B., Zhang, M., Zhang, H., & Sun, J. Z. (2011). *J. Lumin.*, *131*, 1158.
[24] Hohenberg, P., & Kohn, W. (1964). *Phys. Rev.*, *136*, B864.
[25] Becke, A. D. (1993). *J. Chem. Phys.*, *98*, 5648.
[26] Lee, C., Yang, W. T., & Parr, R. G. (1988). *Phys. Rev. B*, *37*, 785.
[27] Hay, P. J., & Wadt, W. R. (1985). *J. Chem. Phys.*, *82*, 270.
[28] Hay, P. J., & Wadt, W. R. (1985). *J. Chem. Phys.*, *82*, 299.
[29] Frisch, M. J., Trucks, G. W., Schlegel, H. B., Scuseria, G. E., Robb, M. A., Cheeseman, J. R., *et al*. (2009). *Gaussian 09*, Gaussian, Inc.: Wallingford, CT.
[30] Hush, N. S. (1958). *J. Chem. Phys.*, *28*, 962.
[31] Marcus, R. A. (1993). *Rev. Mod. Phys.*, *65*, 599.
[32] Marcus, R. A. (1956). *J. Chem. Phys.*, *24*, 966.
[33] Malagoli, M., & Brédas, J. L. (2000). *Chem. Phys. Lett.*, *327*, 13.
[34] Lin, B. C., Cheng, C. P., Ping, Z., & Lao, M. (2003). *J. Phys. Chem. A*, *107*, 5241.
[35] Sakanoue, K., Motoda, M., Sugimoto, M., & Sakaki, S. (1999). *J. Phys. Chem. A*, *103*, 5551.
[36] Lee, Y. Z., Chen, X. W., Chen, S. A., Wei, P. K., & Fann, W. S. (2001). *J. Am. Chem. Soc.*, *123*, 2296.
[37] You, Y., & Park, S. Y. (2005). *J. Am. Chem. Soc.*, *127*, 12438.
[38] Świderek, K., & Paneth, P. (2009). *J. Phys. Org. Chem.*, *22*, 845.
[39] Fantacci, S., De Angelis, F., Sgamellotti, A., Marrone, A., & Re, N. (2005). *J. Am. Chem. Soc.*, *127*, 14144.
[40] Tamayo, A. B., Garon, S., Sajoto, T., Djurovich, P. I., Tsyba, I. M., Bau, R., & Thompson, M. E. (2005). *Inorg. Chem.*, *44*, 8723.
[41] Avilov, I., Minoofar, P., Cornil, J., & De Cola, L. (2007). *J. Am. Chem. Soc.*, *129*, 8247.